Research Article

Journal of PeptideScience

Received: 8 December 2008 Revised: 18 January 2009 Accepted: 21 January 2009 Published online in Wiley Interscience: 10 March 2009

(www.interscience.com) DOI 10.1002/psc.1128

T178 deletion impairs intermolecular interaction of the peptide Nramp1(164–191)

Rong Xue, Shuo Wang, Haiyan Qi, Yuande Song, Shuyan Xiao and Fei Li*

Natural resistance associated macrophage protein 1 (Nramp1), an integral membrane protein with 12 predicted transmembrane domains (TMs), is a divalent cation transporter associated with infectious and autoimmune diseases. A naturally occurring mutation G169D within TM4 of Nramp1 leads to the loss of function, suggesting potential importance of TM4 for the biological function of the protein. In this study, we determine the three-dimensional structure and topology of a synthetic peptide, del(T178), corresponding to Nramp1(164-191) (basically consisting of the putative TM4 of Nramp1) with Thr178 deletion in TFE and SDS micelles using NMR and CD spectroscopic techniques, and compare the results with those of the wildtype peptide. Similarly to the wildtype peptide, the del(T178) peptide still forms an amphiphilic-like α-helical structure in both membrane mimics and is embedded in SDS micelles. Differently, whereas the wild-type peptide forms a helix bundle with the hydrophilic side facing the interior of the bundle, the del(T178) peptide exists as a monomer in the membrane mimics and the hydrophilic side of the helix is located near the interface of SDS micelles. Moreover, a strongly cooperative protonation occurs between intramolecular Asp residues for the del(T178) peptide in SDS micelles, while the cooperative proton binding between intermolecular Asp residues was observed for the wildtype peptide. The difference in the results of the two peptides suggests that the deletion of Thr178 impairs intermolecular interaction of the peptide. **Copyright © 2009 European Peptide Society and John Wiley & Sons, Ltd.**

Supporting information may be found in the online version of this article

Keywords: Nramp1-TM4; Thr178 deletion; NMR; structure; topology

Introduction

Natural resistance associated macrophage protein 1 (Nramp1), also named solute carrier family 11 member 1 (Slc11a1), is a highly glycosylated protein with 12 transmembrane domains (TMs) expressed in macrophages [1]. It belongs to a membrane protein family Nramp, a conserved family of chemiosmotic metal ion transporters. Nramp1 restricts microbial access to essential micronutrients such as iron and manganese within professional phagosomes [2]. It is well established that the divalent cation transport of Nramp1 is pH-dependent, though whether ion and proton are symported or antiported still remains controversial [3].

Nramp1 is involved in defense against intracellular pathogens including *Salmonella typhimurim, Leishmania donovani, and Mycobacterium bovis* [4–7]. A naturally occurring mutation G169D in Nramp1, within the fourth transmembrane domain (TM4), renders mice susceptible to these pathogens [1]. Surprisingly, a naturally disease-causing mutation G185R in Nramp2, another mammalian Nramp protein which shares 78% sequence identity in the hydrophobic core with Nramp1, also locates in TM4 [8,9]. The sequence of TM4 in Nramp1 from mouse [10] is completely identical with that of NRAMP1 from human [11], implying that this domain may play a similar role in Nramp1 and NRAMP1. These facts indicate that TM4 is a region of potential importance to Nramp transport function.

There appears lack of prior knowledge on the structure and assembly of integral Nramp1. We have previously characterized the structures, membrane orientations and self-assemblies of a synthetic peptide corresponding to Nramp1(164–191) (basically consisting of the TM4 of Nramp1) and its G169D mutant in membrane-mimetic environments [12–14]. The wildtype peptide is able to self-associate in model membranes and allows a positively cooperative proton binding of Asp residues from different molecules of assembly, which possibly provides a channel-like pathway for the proton-coupled transport of divalent metal ions. The G169D mutation impairs the entry of metal ions likely by changing the cooperative manner of proton binding or assembling form. In this work, we investigate a peptide corresponding to Nramp1(164–191) with Thr178 deletion in TFE and SDS micelles using CD and NMR techniques. The reasons for studying the del(T178) peptide are based on the following two points: (i) In the previous NMR study for the TM4-related peptides in 1,1,1,3,3,3-hexa-fluoroisopropanol-d_2 aqueous solution, we found that the residues near the C termini of helices (between Phe180 and Leu184) may play an important role for the assembly conformations [12]. To further testify the importance of the C-terminus of helix in regulating self-assembly of the TM4 peptide, we deleted Thr178 that locates at the middle of the peptide. We guessed that if the N-terminal part is not involved in the intermonomer interaction, the peptide aggregate should be kept. In contrast, if the N-terminal part of the peptide also participates in the intermonomer interaction, the aggregate of the peptide

* *Correspondence to: Fei Li, State Key Laboratory of Supramolecular Structure and Materials, Jilin University, 2699 Qianjin avenue, Changchun 130012, People's Republic of China. E-mail: feili@jlu.edu.cn*

State Key Laboratory of Supramolecular Structure and Materials, Jilin University, Changchun 130012, People's Republic of China

Copyright © 2009 European Peptide Society and John Wiley & Sons, Ltd.

should be weakened or destroyed as the relative arrangement of the residues before and after deletion point is changed. (ii) On the basis of known membrane protein structures, polar residue Thr is likely to play a role in helix–helix association and hence in the folding of multispanning membrane proteins [15,16]. Therefore, the study of the peptide may provide us information on the relationship between the structure and assembly. The results indicate that the deletion of Thr178 impairs the intermolecular interaction.

Materials and Methods

Sample Preparation

The 27-mer peptide with a sequence of Arg^{1}-Ile^{2}-Pro^{3}-Leu^{4}-Trp^{5}-Gly^{6}-Gly^{7}-Val^{8}-Leu^{9}-Ile^{10}-Thr^{11}-Ile^{12}-Val^{13}-**Asp^{14}-Phe^{16}**-Phe^{17}-Phe^{18}-Leu^{19}-Phe^{20}-Leu^{21}-Asp^{22}-Asn^{23}-Tyr^{24}-Gly^{25}-Leu^{26}-Arg^{27}-Lys^{28} (the residue numbers are identical with those in the wildtype peptide [13]), corresponding to Nramp1(164–191) with Thr178 (Thr15 in the peptide) deletion, assigned as del(T178), was prepared by solid-phase synthesis and purified by HPLC on a Zorbax SB Phenyl reverse phase column using 0.1% TFA/water and 0.1% TFA/acetonitrile as solvents (Biopeptide CO. LLC. USA). Purity was above 95%, evaluated by both HPLC and mass spectrometry. SDS-d_{25} (98%), D_2O (99.8%), methanol-d_4 (99.6%) and TFE-d_2 (98%) were purchased from Cambridge Isotope Laboratories. TFE (99.8%) and HFIP (99.5%) were purchased from Acros Organics. 16-doxylstearic acid (16-DSA) and SDS (99%) were obtained from Sigma. All chemicals were used as purchased, without further treatment.

The sample containing the peptide in SDS micellar solution was prepared using a method described previously [13]. Briefly, HFIP solution of the peptide was mixed with aqueous solution of SDS or SDS-d_{25}. The mixture was further diluted by addition of H_2O and lyophilized overnight. The resulting powder of the peptide/SDS mixture was dissolved in 0.4 mL of H_2O to obtain the concentration of 20 μM peptide in 10 mM SDS, while the powder of the peptide/SDS-d_{25} mixture was dissolved in 0.6 mL of H_2O/D_2O (90%/10%) mixture to obtain the concentration of 2 mM peptide in 240 mM SDS-d_{25}. The pH was adjusted by addition of a small amount of NaOH or HCl solution. The 16-DSA was added as a solution to the least amount of methanol-d_4 to give a molar ratio of detergent to spin label of 60 : 1.

CD Measurements

Far-UV CD spectra were recorded from 260 to 190 nm with a Jasco J-810 spectropolarimeter. Spectra were acquired at room temperature using 0.5-mm path length cell, averaged three scans, at a scan speed of 50 nm/min, bandwidth of 1.0 nm, response time of 0.25 s, and 0.1 nm data pitch. The solvent spectrum was subtracted from the sample spectrum. The secondary structure contents were estimated by the CDPro software package [17] using the program SELCON3 with 43-protein set.

NMR Measurements

The ^{1}H-NMR spectra were acquired at 298 K and 310 K in TFE and SDS micelles, on a Bruker Avance 500 spectrometer using a 5-mm TBI triple resonance inverse probehead equipped with a z-axis gradient coil. Two-dimensional TOCSY and NOESY were collected using the WATERGATE technique, with a mixing time of 100 ms and 200 ms, respectively. Typical data were 2048 complex data points, 72–112 transients, and 256 increments. All chemical shifts were referenced to TSP [sodium salt of 3-(trimethylsilyl)-propionate-2, 2, 3, 3-d_4]. The spectra were processed using standard Bruker software (XWINNMR Version 3.5) and analyzed using the software SPARKY [18]. The NOE intensities and chemical shifts were extracted using SPARKY and served as an input for the structure calculation.

Proton chemical shift titration data were fitted to a modified Hill equation [19]

$$\delta(\mathrm{pH}) = \frac{\delta_{\mathrm{base}} + \delta_{\mathrm{acid}} \times 10^{n(\mathrm{pH_m}-\mathrm{pH})}}{1 + 10^{n(\mathrm{pH_m}-\mathrm{pH})}} \quad (1)$$

the acidic (δ_{acid}) and basic (δ_{base}) plateaus, Hill coefficient (n) and pH midpoint ($\mathrm{pH_m}$) were left as floating parameters during the nonlinear least square analysis carried out using Origin v6.

Structure Calculation

The three-dimensional structures of the peptide in membrane-mimetic environments were calculated with the program CYANA (version 1.0.6) [20] using a standard simulated annealing protocol. On the basis of the upper limits of the distance restraints obtained from NOEs using the macro CALIBA, a systematic analysis of the local conformation around the C_α atom of each residue, including the dihedral angles ϕ, ψ, χ^1 and χ^2, was performed using the macro GRIDSEARCH as implemented in CYANA. Structure calculations were started from 200 conformers with random torsion angle values. The 20 conformers with the lowest final CYANA target function values were further refined by energy minimization employing the AMBER7 program [21,22] under the force field of Cornell *et al* [23] using a generalized Born solvent model. The resulting structures were viewed and analyzed by MOLMOL [24] and PROCHECKNMR [25].

Diffusion-Ordered Spectroscopy (DOSY) Measurements

All DOSY spectra were acquired at 298 K. Gradient strength was calibrated using HDO signal in D_2O. The diffusion coefficient of the peptide was measured with bipolar pulse pair stimulated echo (BPPSTE) sequence using WATERGATE technique. Diffusion time (Δ) was 50 ms. Durations of pulse gradients (δ) were 2.8 and 3.25 ms for 2 and 0.5 mM of peptide, respectively. Data were acquired with eight scans.

To estimate the viscosity of the peptide, the diffusion coefficient of TFE in the TFE/peptide samples was measured separately using the sequence of pulsed field gradient stimulated echo (STE) without water suppression, with Δ of 50 ms, δ of 3.1 ms for 0.5 mM sample and 3.2 ms for 2 mM sample, and scans of eight.

The dynamic viscosities (η) of TFE solutions and the molecular mass (M) of the peptides in TFE solutions were estimated by the method previously used [26] based on Stokes–Einstein relation and the diffusion coefficients of the peptides measured by DOSY experiments.

Results and Discussion

Secondary Structure Analyses by CD

The secondary structure of the peptide del(T178) in TFE and SDS micelles were probed by far-UV CD spectroscopy (Figure 1). All

 Copyright © 2009 European Peptide Society and John Wiley & Sons, Ltd.

Journal of PeptideScience

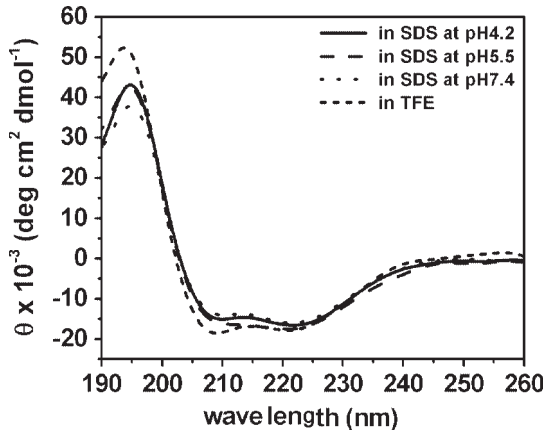

Figure 1. CD spectra for 20-μM del(T178) peptide in pure TFE and 10-mM SDS at various pH values at room temperature.

CD spectra were characterized by a negative 222-nm band due to the peptide n $-\pi^*$ transition, a negative 208-nm and a positive 192-nm band due to $\pi-\pi^*$ transition exciton splitting of the peptide [27]. This strongly suggests the existence of a significant population of α-helical conformers. The α-helical contents of the del(T178) peptide estimated by SELCON3 from CDPro software are *ca.* 71.2% in TFE, and 66.5% at pH 4.2, 66.4% at pH 5.5 and 59.8% at pH 7.4 in SDS micelles.

NMR Structures

The ^{1}H resonance assignment was carried out based on the Wüthrich procedure [28]. Basically, 2D TOCSY was used to identify the spin system of the individual amino acid residues, and NOESY was used to establish backbone sequential connectivities. Figure 2A and B give partial Hα-HN NOESY spectra in TFE and SDS micelles, respectively, with assignments labeled. The presence of medium range NOEs (such as Hα_i-HN$_{i+3}$, Hα_i-Hβ_{i+3} and Hα_i-HN$_{i+4}$) and strong sequential NOEs between amide protons in NOE connectivities and series of −1 in chemical shift index (CSI) shown in Figure 2C and D assumes α-helical conformations from Trp5-Gly25 in TFE and Val8-Gly25 in SDS at pH 5.5 for the del(T178) peptide, which are in good agreement with the results of CD.

Three-dimensional structures of the del(T178) peptide in TFE and SDS micelles at different pH values were determined from distance constraints derived from 2D NOESY combined with the molecular dynamics simulated annealing approach and energy minimizing. The structural statistics for 20 energy-minimized structures with the lowest target functions are summarized in Table 1. Figure 3A and B show the superposition of 20 energy-minimized structures of the peptide in TFE and SDS micelles at pH 5.5. The overall structures are similar in both media with highly defined α-helical conformations in their middle portions, flanked by a flexible N-terminus and a relatively ordered C-terminus. However, the helical regions are slightly different which spans from Gly6 to Leu26 in TFE and Val8 to Gly25 in SDS micelles at pH 5.5. A small amount of increase in helical length of the peptide in TFE may result from the stronger ability of the organic solvent to induce an α-helical structure [29]. In SDS micelles, the helical structure of the peptide is conserved at different pH values, pH 4.2, 5.5 and 7.4 (Figure 3C), which is evidenced by NOE connectivities (Figure S1, supporting information) and calculated results.

Location of the Peptide in SDS Micelles

The location of a peptide in membrane and extent of solvent exposure for each residue can be determined using paramagnetic additives. The detergent-like paramagnetic probe, 16-DSA, and paramagnetic metal-ion, Mn^{2+}, can be used to probe the residues near the center of SDS micelles [30] and the residues situated in the aqueous phase or at the surface of detergent micelles, respectively [31,32]. Therefore, the information about peptide topology in SDS micelles can be gained from 16-DSA and Mn^{2+} experiments. In this study, the paramagnetic broadening effects were investigated by comparing two-dimensional NOESY spectra in the presence and absence of the paramagnetic agent.

Figure 4A illustrates the residual relative intensities of the Hα-HN cross-peaks from NOESY spectra in the presence of 4 mM 16-DSA in SDS micelles at pH 5.5. The NMR signals of residues Trp5, Val13 and Phe17 are broadened significantly, while the rest of the residues are little affected. Since the radical group of 16-DSA is found near the center of the micelles and selectively broadened the NMR signals of the residues close to the center of the micelles [30], the results indicate that the peptide is inserted into SDS micelles and the residues Trp5, Val13 and Phe17 locate near the hydrophobic core of SDS micelles.

To further determine whether some parts of the del(T178) peptide are exposed to aqueous phase, Mn^{2+} was added into the peptide/SDS aqueous solution. As shown in Figure 4B, in the presence of 0.1 mM Mn^{2+} at pH 5.5, the intensities of Hα-HN cross-peaks from residues Asp14 and Asp22 are completely quenched and that of Asn23 is also reduced largely, however, the other residues are less affected. This implies that the most region of the peptide is embedded in SDS micelles and water unaccessible, while the residues Asp14, Asp22 and Asn23 are water accessible.

pH Dependence of Proton Chemical Shifts in SDS Micelles

pH Dependence of the proton chemical shifts from backbone amides and carboxylate side chains is a good probe to identify residue–residue interactions in polypeptides [33]. The pH mid-point (pH_m) and so-called Hill coefficient (*n*) are the essential parameters in pH dependence analysis. The pH_m values of the backbone amides and carboxylate side chains in folded proteins reflect the electrostatic surroundings of the residues [34–36], which may be increased in an apolar surrounding or decreased in a polar surrounding. The Hill coefficients provide an indication of cooperativity [33]. The *n* values larger and less than 1 correspond to the positive and negative cooperativities of the proton binding, respectively, by which the protonation of one carboxylate is favorable (positive cooperativity) or unfavorable (negative cooperativity) to the protonation of others. Isolated ionizable residues would be expected to have the coefficient close to unity [37].

Figure 5 illustrates the pH dependence of the proton chemical shifts of the residues with the titration shift $|\Delta\delta|$ larger than 0.1 ppm, including Asp14 (Hβ and HN), and Val13, Leu21, Asp22 and Asn23 (HN). The data were fitted in terms of Eq. 1, as illustrated by the curves in the figure, and the titration parameters pH_m and Hill coefficient *n* were obtained (Table 2). The overall Hill coefficients of these residues are larger than 1, consistent with positive cooperativity in proton binding. Moreover, the pH_m values obtained from either Hβ or HN titration curves of these residues are larger than the standard value 3.9 measured by Bundi and Wuthrich in aqueous medium [35], indicating that the residues locate at an environment less polar than water. It is noteworthy that all these residues have approximately identical pH_m and *n* values

 Copyright © 2009 European Peptide Society and John Wiley & Sons, Ltd.

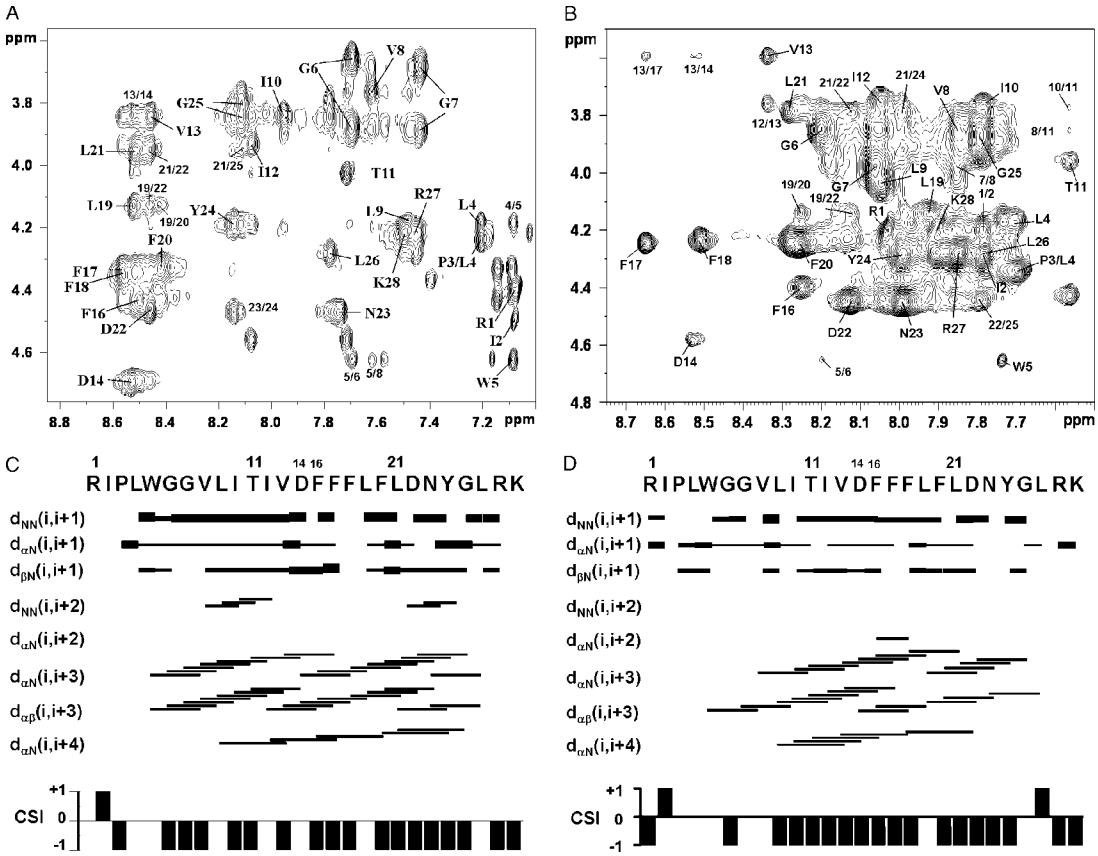

Figure 2. Hα-HN region of the NOESY spectra with assignments and NOE connectivities, as well as CSI for 2-mM del(T178) peptide in TFE-d_2 (A and C) and in 240-mM SDS-d_{25} at pH 5.5 (B and D), 310 K.

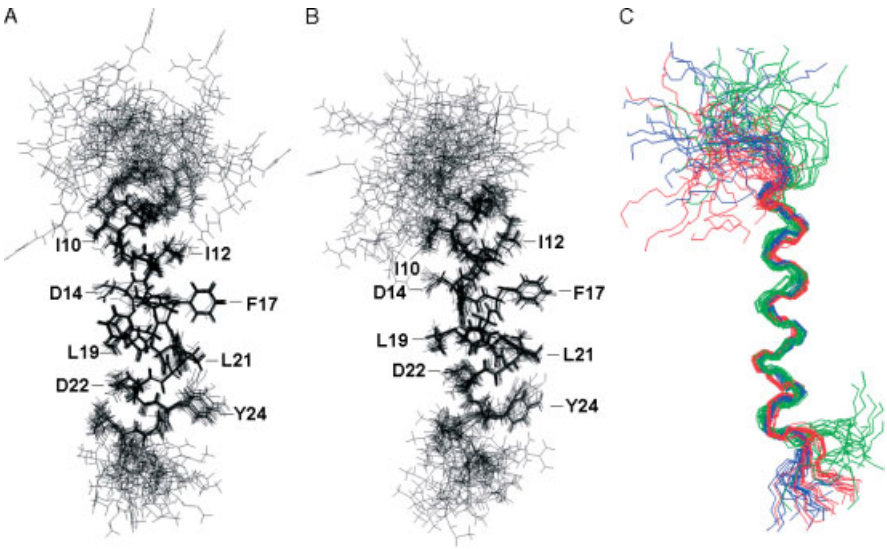

Figure 3. Superposition of the 20 energy-minimized structures of the del(T178) peptide in TFE-d_2 (A) and SDS-d_{25} micelles at pH 5.5 (B) and comparison of the structures for the del(T178) peptide in SDS-d_{25} micelles at pH 4.2 (blue), 5.5 (red) and 7.4 (green) (C), 310 K.

within the experimental error. Obviously, the titration parameters of nonionizable residue Val13 reflect the effect of the charge state of neighboring ionizable residue Asp14, and those of Leu21 and Asn23 arise largely from effect of the electrostatic surrounding of Asp22. Interestingly, Asp14 and Asp22 that are 7-residue distant in the del(T178) peptide show similar pH_m and n values. This implies that the two residues may be involved in the remote interaction and thus a cooperative proton association ($n > 1$).

Diffusion Coefficient Measurements in TFE

The DOSY spectra of the del(T178) peptide were measured in pure TFE-d_2 at concentrations of 2 and 0.5 mM (Figure S2,

 Copyright © 2009 European Peptide Society and John Wiley & Sons, Ltd.

Journal of PeptideScience

Table 1. Structural statistics of the peptide in SDS micelles and TFE at 310 K

	SDS			
	pH 4.2	pH 5.5	pH 7.4	TFE
Average target functions (Å^2)	0.27 ± 0.07	0.23 ± 0.06	0.18 ± 0.04	0.29 ± 0.03
Number of nonredundant distance restraints	302	291	281	305
Intraresidual ($\|i-j\|=0$)	136	126	124	127
Sequential ($\|i-j\|=1$)	80	83	82	84
Medium ($\|i-j\|\leq 4$)	86	82	75	94
Long range ($\|i-j\|>4$)	0	0	4	0
Average sum of distance restraint violations	1.9 ± 0.3	1.9 ± 0.3	1.6 ± 0.3	2.3 ± 0.2
Average maximum distance restraint violation	0.22 ± 0.05	0.26 ± 0.10	0.18 ± 0.05	0.18 ± 0.02
Average sum of torsion angle restraint violations (°)	0.1 ± 0.2	0.0 ± 0.0	0.0 ± 0.0	0.0 ± 0.0
Average maximum of torsion angle restraint violation (°)	0.09 ± 0.24	0.00 ± 0.00	0.01 ± 0.03	0.00 ± 0.00
AMBER energy (kcal mol^{-1})	−1117.93 ± 0.70	−1108.46 ± 1.39	−1115.9 ± 0.45	−1133.24 ± 0.41
R.m.s. deviation from the mean structure (Å)				
All residues				
Backbone heavy atoms	2.57 ± 0.71	2.64 ± 0.75	2.92 ± 0.76	2.79 ± 0.82
All heavy atoms	3.86 ± 0.86	3.84 ± 0.86	4.21 ± 0.90	4.00 ± 0.94
Residues for helical span				
Backbone heavy atoms	0.40 ± 0.25	0.56 ± 0.23	0.59 ± 0.23	0.43 ± 0.17
All heavy atoms	1.12 ± 0.31	1.24 ± 0.24	1.27 ± 0.26	1.02 ± 0.24
Ramachandran plot statistics (at each helical span)				
Residues in most favored region (%)	95	86.9	94.1	100
Residues in additionally allowed region (%)	5	13.1	5.9	0
Residues in generously allowed region (%)	0	0	0	0
Residues in disallowed region (%)	0	0	0	0

R.m.s. deviation, root mean square deviation.

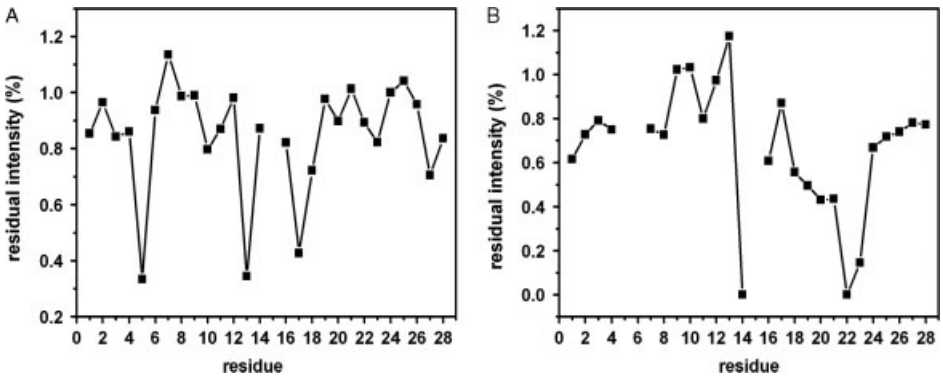

Figure 4. The residual intensities of the Hα-HN cross-peaks for the del(T178) peptide in SDS-d_{25} micelles in presence of 16-DSA (A) and Mn^{2+} (B) at pH 5.5, 310 K.

supporting information). The diffusion coefficients of the peptide at two concentrations have little difference (2.16×10^{-10} m^2 s^{-1} for 2 mM sample and 1.86×10^{-10} m^2 s^{-1} for 0.5 mM sample). The similar viscosities of the two solutions were also obtained (1.13×10^{-3} N s m^{-2} for 2 mM peptide and 1.17×10^{-3} N s m^{-2} for 0.5 mM peptide) by the diffusion coefficients of TFE in the two concentrations of samples (8.22×10^{-10} m^2 s^{-1} for 2 mM peptide and 7.89×10^{-10} m^2 s^{-1} for 0.5 mM peptide). From the diffusion coefficients of the peptide and the viscosities of the solution, the molecular masses of the peptide in TFE were estimated to be ~1.6 and ~2.2 kDa for 2 and 0.5 mM peptide, respectively. The molecular mass of the peptide obtained from the MS analysis is 3.2 kDa. The DOSY experiment demonstrates that the del(T178) peptide exists in TFE solution as monomer.

Comparison of the del(T178) Peptide with Wildtype Peptide

Point mutations and deletions in proteins usually cause functional disorders or diseases. The biochemical and biophysical researches on proteins and peptides with naturally occurring or artificial point mutations and deletions could help us to understand the mechanisms of biomolecules. For example, the investigations on a series of deletion and substitution mutants of Loop 7 connecting β stands 12 and 13 of calcineurin revealed the importance of Loop 7 for calcineurin activity [38–41]. In the present study, we focus our interest on the peptide corresponding to Nramp1(164–191)

 Copyright © 2009 European Peptide Society and John Wiley & Sons, Ltd.

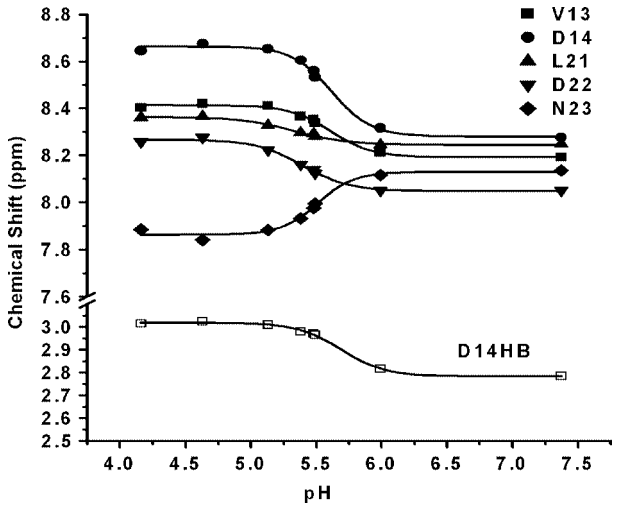

Figure 5. pH titration of protons for the del(T178) peptide in SDS-d_{25} micelles at 310 K.

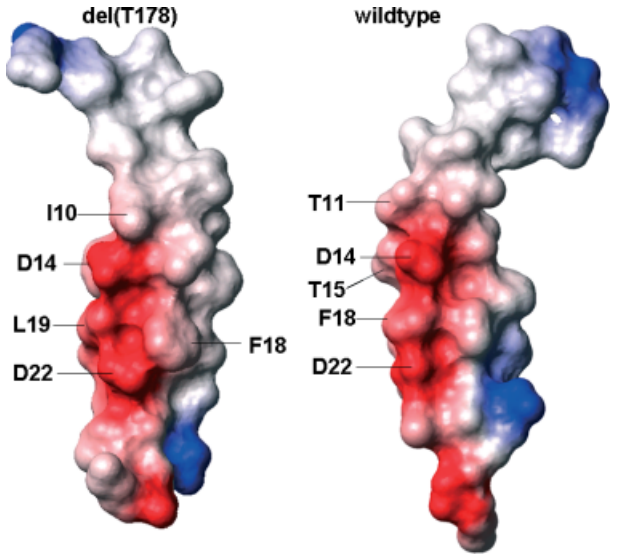

Figure 6. Surface plots of the del(T178) peptide and the wildtype peptide in SDS micelles.

Table 2. pH Dependence of titratable residues and some amide reporters

	Residue	pH_m	n	$\Delta\delta$ (ppm)[a]
Backbone amide (HN)	V13	5.61 ± 0.04	2.73 ± 0.50	−0.22
	D14	5.62 ± 0.04	2.88 ± 0.52	−0.38
	L21	5.33 ± 0.04	2.10 ± 0.45	−0.12
	D22	5.39 ± 0.03	2.41 ± 0.43	−0.22
	N23	5.51 ± 0.03	3.15 ± 1.11	0.27
Carboxylate sidechain (Hβ)	D14	5.69 ± 0.02	2.58 ± 0.19	−0.24

[a] $\Delta\delta = \delta_{base} - \delta_{acid}$.

with Thr178 deletion and expect to get more knowledge about Nramp1-TM4 through comparing the structure and topology of the del(T178) peptide with its wildtype peptide.

In the aspect of three-dimensional structure, although the deletion of Thr178 (corresponding to Thr15 in the wildtype peptide) does not abrogate the ability of the peptide to form a helix with an amphiphilic-like residue arrangement, four residues Thr15–Phe18 that provide amide H to form H-bonds with carbonyl O of the residues Thr11–Asp14, respectively, in helix of the wildtype peptide, are displaced by the residues Phe16–Leu19 for the del(T178) peptide. The displacement of these residue pairs in helix decreases the distance between Asp14 and Asp22 in the del(T178) peptide compared with the wildtype peptide, and the aromatic ring of Phe18 that locates at the middle of Asp14 and Asp22 in the helical structure of wildtype peptide is moved aside in the del(T178) peptide (Figure 6), which are in favor of the interaction between Asp14 and Asp22 within the molecule.

The effects of the paramagnetic probes 16-DSA and Mn^{2+} ion on the intensities of proton NMR signals reveal that the del(T178) peptide is also totally embedded into SDS micelles, as observed for the wildtype peptide. However, the pH titration experiments of the del(T178) peptide give pH_m values of some residues that are smaller than the corresponding values of the wildtype peptide (except for Asp22), but close to the value of Asp22 of the wildtype peptide that locates near the interface of SDS micelles [13], suggesting that the buried position of the del(T178) peptide is moved towards the surface of micelles relative to the deeper embedding of the wildtype peptide in the interior of SDS micelles. The shallower embedding of the del(T178) peptide in SDS micelles allows the anionic sidechain of Asp14 to extend towards the surface of the micelles, which may lead to a severe quenching of Asp14 by Mn^{2+}.

The diffusion measurements reveal that the del(T178) peptide exists as a monomer in TFE even at 2 mM concentration where assembly was observed for the wildtype peptide. The pH titration experiments of the del(T178) peptide in SDS micelles seem to provide further support for the result in TFE. The positively cooperative proton binding of Asp22 and Asp14 in the del(T178) peptide occurs within monomer. In contrast, for the wildtype peptide, Asp22 is isolated ($n = 1$), and Asp14 showed the positively cooperative protonation ($n > 1$) which was attributed to the intermolecular interaction of the peptide assembly [12,13]. The self-assembly was also observed in the previous studies on the model peptides corresponding to the fourth TM of Nramp2 in model membranes [26,42–44]. The disassociation of the del(T178) peptide in both TFE and SDS micelles suggests that the Thr178 deletion could impair intermolecular interaction of the peptide. A possible explanation is that the residue Thr178 is involved in the helix–helix interactions of the wildtype peptides (on the basis of known membrane protein structures, polar residue threonine is likely to play a role in helix–helix association and hence in the folding of multispanning membrane proteins [45]) or the residue is essential for forming a helical structure in which residues are arranged favorably to self-assembly. As observed by our previous study, the wildtype peptide adopts an α-helical structure with the polar residues Thr11, Asp14, Thr15, and Asp22 located in the same side and apolar residues in the other side. These polar residues may face to the interior of the helix bundle to avoid causing unfavorable free energy in hydrophobic environment of the micelles. In the del(T178) peptide, the missing of residue Thr15 leads to a change in the residue arrangement of the hydrophilic side, from Thr11, Asp14, Thr15, Phe18 and Asp22 to Ile10, Asp14, Leu19 and Asp22 (Figure 6), which may disrupt or decrease the affinity of hydrophilic side of the peptide.

 Copyright © 2009 European Peptide Society and John Wiley & Sons, Ltd.

In conclusion, although the deletion of the residue Thr178 does not eliminate the predominately α-helical conformation in model membranes, it impairs the intermolecular interaction and alters the cooperativity in proton binding of Asp14 and Asp22. As a monomer, the del(T178) peptide is embedded in SDS micelles with the hydrophobic side facing the hydrophobic core of the micelles and the hydrophilic-like side approaching the interface of the micelles. This study suggests a potential role of the polar residue Thr178 for the orientation and intermolecular interaction of Nramp1-TM4.

Supporting information

Supporting information may be found in the online version of this article.

Acknowledgement

This work was financially supported by the NSFC (20673043).

References

1 White JK, Stewart AS, Popoff JF, Wilson S, Blackwell JM. Incomplete glycosylation and defective intracellular targeting of mutant solute carrier family 11 member 1 (Slc11a1). *Biochem. J.* 2004; **382**: 811–819.
2 Cellier MF, Courville P, Campion C. Nramp1 phagocyte intracellular metal withdrawal defense. *Microbes Infect.* 2007; **9**: 1662–1670.
3 Nevo Y, Nelson N. The NRAMP family of metal-ion transporters. *Biochim. Biophys. Acta* 2006; **1763**: 609–620.
4 Vidal SM, Malo D, Vogan K, Skamene E, Gros P. Natural resistance to infection with intracellular parasites: isolation of a candidate for Bcg. *Cell* 1993; **73**: 469–485.
5 Blackwell JM, Searle S, Mohamed H, White JK. Divalent cation transport and susceptibility to infectious and autoimmune disease: continuation of the Ity/Lsh/Bcg/Nramp1/Slc11a1 gene story. *Immunol. Lett.* 2003; **85**: 197–203.
6 Blackwell JM, Searle S. Genetic regulation of macrophage activation: understanding the function of Nramp1 (=Ity/Lsh/Bcg). *Immunol. Lett.* 1999; **65**: 73–80.
7 Blackwell JM, Searle S, Goswami T, Miller EN. Understanding the multiple functions of Nramp1. *Microbes Infect.* 2000; **2**: 317–321.
8 Fleming MD, Trenor CCI, Su MA, Foernzler D, Beier DR, Dietrich WF, Andrews NC. Microcytic anaemia mice have a mutation in Nramp2, a candidate iron transporter gene. *Nat. Genet.* 1997; **16**: 383–386.
9 Su MA, Trenor CC, Fleming JC, Fleming MD, Andrews NC. The G185R mutation disrupts function of the iron transporter Nramp2. *Blood* 1998; **92**: 2157–2163.
10 Cellier M, Prive G, Belouchi A, Kwan T, Rodrigues V, Chia W, Gros P. Nramp defines a family of membrane proteins. *Proc. Natl. Acad. Sci. U.S.A.* 1995; **92**: 10089–10093.
11 Feng J, Li Y, Hashad M, Schurr E, Gros P, Adams LG, Templeton JW. Bovine natural resistance associated macrophage protein 1 (Nramp1) gene. *Genome Res.* 1996; **6**: 956–964.
12 Xue R, Wang S, Wang C, Zhu T, Li F, Sun H. HFIP-induced structures and assemblies of the peptides from the transmembrane domain 4 of membrane protein Nramp1. *Biopolymers* 2006; **84**: 329–339.
13 Xue R, Wang S, Qi H, Song Y, Wang C, Li F. Structure analysis of the fourth transmembrane domain of Nramp1 in model membranes. *Biochem. Biophys. Acta* 2008; **1778**: 1444–1452.
14 Xue R, Wang S, Qi H, Song Y, Xiao S, Wang C, Li F. Structure and topology of Slc11a1(164–191) with G169D mutation in membrane-mimetic environments. *J. Struct. Biol.* 2009; **165**: 27–36.
15 Arkin IT, Brunger AT. Statistical analysis of predicted transmembrane α-helices. *Biochim. Biophys. Acta* 1998; **1429**: 113–128.
16 Nyholm TKM, Őzdirekcan S, Killian JA. How protein transmembrane segments sense the lipid environment. *Biochemistry* 2007; **46**: 1457–1465.
17 Sreerama N, Woody RW. Estimation of protein secondary structure from circular dichroism spectra: comparison of CONTIN, SELCON, and CDSSTR methods with an expanded reference set. *Anal. Biochem.* 2000; **287**: 252–260.
18 Goddard TD, Kneller DG. *SPARKY 3*. University of California: San Francisco, CA, 2001.
19 Markley JL. Observation of histidine residues in proteins by means of nuclear magnetic resonance spectroscopy. *Acc. Chem. Res.* 1975; **8**: 70–80.
20 Güntert P, Mumenthaler C, Wüthrich K. Torsion angle dynamics for NMR structure calculation with the new program DYANA. *J. Mol. Biol.* 1997; **273**: 283–298.
21 Pearlman DA, Case DA, Caldwell JW, Ross WS, Cheatham TE, DeBolt S, Ferguson D, Seibel G, Kollman P. AMBER, a package of computer programs for applying molecular mechanics, normal mode analysis, molecular dynamics and free energy calculations to simulate the structural and energetic properties of molecules. *Comput. Phys. Commun.* 1995; **91**: 1–41.
22 Case DA, Pearlman DA, Caldwell JW, Cheatham TE III, Wang J, Ross WS, Simmerling CL, Darden TA, Merz KM, Stanton RV, Cheung AI, Vincent JJ, Crowley M, Tsui V, Gohike H, Radmer RJ, Duan Y, Pitera J, Massova I, Seibel GL, Singh UC, Weiner PK, Kollman PA. *AMBER 7*. University of California: San Francisco, 2002.
23 Cornell WD, Cieplak P, Bayly CI, Gould IR, Merz KM Jr, Ferguson DM, Spellmeyer DC, Fox T, Caldwell JW, Kollman PA. A second generation force field for the simulation of proteins, nucleic acids, and organic molecules. *J. Am. Chem. Soc.* 1995; **117**: 5179–5197.
24 Koradi R, Billeter M, Wüthrich K. MOLMOL: a program for display and analysis of macromolecular structures. *J. Mol. Graphics* 1996; **14**: 51–55.
25 Laskowski RA, Rullmann JA, MacArthur MW, Kaptein R, Thornton JM. AQUA and PROCHECK-NMR: programs for checking the quality of protein structures solved by NMR. *J. Biomol. NMR* 1996; **8**: 477–486.
26 Li F, Li H, Hu L, Kwan M, Chen G, He Q-Y, Sun H. Structure, assembly and topology of the G185R mutant of the fourth transmembrane domain of divalent metal transporter. *J. Am. Chem. Soc.* 2005; **127**: 1414–1423.
27 Sreerama N, Woody RW. Circular dichroism of peptides and proteins. In *Circular Dichroism: Principles and Applications*, Berova N, Nakanishi K, Woody RW (eds). Wiley: New York, 2000; 601–620.
28 Wüthrich K. *NMR of Proteins Nucleic Acids*. John Wiley and Sons: New York, 1986.
29 Banerjee T, Kishore N. Does the anesthetic 2,2,2-trifluoroethanol interact with bovine serum albumin by direct binding or by solvent-mediated effects? A calorimetric and spectroscopic investigation. *Biopolymers* 2005; **78**: 78–86.
30 Papavoine CHM, Konings RNH, Hilbers CW, van de Ven FJM. Location of M13 coat protein in sodium dodecyl sulfate micelles as determined by NMR. *Biochemistry* 1994; **33**: 12990–12997.
31 Lindberg M, Jarvet J, Langel U, Gräslund A. Secondary structure and position of the cell-penetrating peptide transportan in SDS micelles as determined by NMR. *Biochemistry* 2001; **40**: 3141–3149.
32 Lindberg M, Gräslund A. The position of the cell penetrating peptide penetratin in SDS micelles determined by NMR. *FEBS Lett.* 2001; **497**: 39–44.
33 Pujato M, Bracken C, Mancusso R, Cataldi M, Tasayco ML. pH dependence of amide chemical shifts in natively disordered polypeptides detects medium-range interactions with ionizable residues. *Biophys. J.* 2005; **89**: 3293–3302.
34 Laurents DV, Huyghues-Despointes BMP, Bruix M, Thurlkill RL, Schell D, Newson S, Grimsley GR, Shaw KL, Treviño S, Rico M, Briggs JM, Antosiewicz JM, Scholtz M, Pace CN. Charge-charge interactions are key determinants of the pK values of ionizable groups in ribonuclease Sa (pI = 3.5) and a basic variant (pI = 10.2). *J. Mol. Biol.* 2003; **325**: 1077–1092.
35 Bundi A, Wüthrich K. Use of amide ^{1}H-NMR titration shifts for studies of polypeptide conformation. *Biopolymers* 1979; **18**: 299–311.
36 Oliveberg M, Arcus VL, Fersht AR. pKa values of carboxyl groups in the native and denatured states of barnase: the pK_a values of the denatured state are on average 0.4 units lower than those of model compounds. *Biochemistry* 1995; **34**: 9424–9433.
37 Song J, Laskowski M, Qasim MA, Markley JL. NMR determination of pKa values for Asp, Glu, His, and Lys mutants at each variable contiguous enzyme-inhibitor contact position of the turkey ovomucoid third domain. *Biochemistry* 2003; **42**: 2847–2856.
38 Wei Q, Lee EYC. Mutagenesis of the L7 Loop Connecting β Strands 12 and 13 of Calcineurin: Evidence for a Structural Role in Activity Changes. *Biochemistry* 1997; **36**: 7418–7424.

 Copyright © 2009 European Peptide Society and John Wiley & Sons, Ltd.

39 Liu P, Huang C, Wang HL, Zhou K, Xiao FX, Wei Q. The importance of Loop 7 for the activity of calcineurin. *FEBS Lett.* 2004; **577**: 205–208.
40 Yan LJ, Wei Q. High activity of the calcineurin A subunit with a V314 deletion. *Biol. Chem.* 1999; **380**: 1281–1285.
41 Wang H, Yao S, Lin W, Du Y, Xiang B, He S, Huang C, Wei Q. Different roles of Loop 7 in inhibition of calcineurin. *Biochem. Biophys. Res. Commun.* 2007; **362**: 263–268.
42 Li H, Li F, Sun H, Qian ZM. Membrane-inserted conformation of transmembrane domain 4 of divalent-metal transporter. *Biochem. J.* 2003; **372**: 757–766.
43 Li H, Li F, Qian ZM, Sun H. Structure and topology of the transmembrane domain 4 of the divalent metal transporter in membrane-mimetic environments. *Eur. J. Biochem.* 2004; **271**: 1938–1951.
44 Li H, Li F, Kwan M, He Q, Sun H. NMR structures and orientation of the fourth transmembrane domain of the rat divalent metal transporter (DMT1) with G185D mutation in SDS micelles. *Biopolymers* 2005; **77**: 173–183.
45 Zhou FX, Merianos H, Brunger AT, Engelman DM. Polar residues drive association of polyleucine transmembrane helices. *Proc. Natl. Acad. Sci. U.S.A.* 2001; **98**: 2250–2255.

 Copyright © 2009 European Peptide Society and John Wiley & Sons, Ltd.